Journal of Structural Geology, Vol. 1, No. 4, 1979, pp. 259 to 273.
Pergamon Press Ltd. 1980. Printed in Great Britain.

Texture and fabric studies across the Kishorn Nappe, near Kyle of Lochalsh, Western Scotland

M. P. Coward and J. S. Whalley*

Department of Earth Sciences, University of Leeds, Leeds LS2 9JT, England

(*Received* 16 *March* 1979; *accepted in revised form* 14 *November* 1979)

Abstract—The progressive development of mylonitic fabrics in a series of Torridonian sandstones and shales has been studied along traverses across the Kishorn Nappe. The fabrics developed have been investigated using the following techniques.

1. Optical examination of thin sections.
2. Measurements of the anisotropy of magnetic susceptibility.
3. X-ray texture goniometry.

The results are used in support of a proposed deformation history of the area and the relative advantages of the techniques used are discussed.

The early deformation was well lubricated with layer-parallel sliding and little internal deformation of the rocks, except for development, in the east, of a layer-parallel penetrative fabric with an extension direction to the ESE. This deformation produced a westward facing isoclinal anticline and a recumbent syncline in the Torridonian rocks which became at least partly decoupled from the basement.

The important phases of fabric development post date this folding. In the west the sandstones developed a spaced, pressure solution cleavage, but in the east the grain shape fabric has been produced by both dislocation and diffusion processes. The shales reveal more details of the deformation episodes than do the sandstones and thus show different fabric intensities and orientations when measured by magnetic and X-ray techniques.

The magnetic anisotropy technique of fabric analysis gives a rapid method of mapping the deformation domains formed by different deformation mechanisms and intensities. However, the rocks carry several magnetic components and these have different anisotropy tensors and different responses to deformation, also, measurements made at high fields (5 kOe) give magnitudes and orientations of the magnetic anisotropy tensor which are different from those made at low fields. It is concluded that it is not possible to relate variations in the magnitude and shape of the magnetic anisotropy ellipsoid quantitatively to the deformation.

Chlorite and muscovite fabrics measured by X-ray techniques show variations in intensity and orientation similar to those of the magnetic anisotropy ellipsoid due to paramagnetic minerals. However, the data demonstrate the difficulty of correlating this fabric intensity with deformation intensity where there has been a change in deformation mechanisms with time and space.

INTRODUCTION

The Kishorn Nappe forms one of the lowermost units of the Moine thrust zone at the north-west edge of the Caledonian fold belt of north-west Scotland, and has been described by Peach *et al.* (1907), Bailey (1939, 1955) and more recently by Kanungo (1956) and Barber (1965). In the Lochalsh region of Skye and the Scottish mainland (Fig. 1) the western part of the nappe consists of thrust, but internally undeformed Torridonian sediments. In the east these sediments are overturned, intensely deformed and overlain by mylonites and crushed Lewisian gneiss of the Balmacara nappe. Peach *et al.* (1907) first described how, as traced eastwards towards the more deformed zone, quartz grains within the Torridonian rocks first developed strain shadows and then became lenticular, the grains being replaced by micro-crystalline aggregates, until in the east 'the grain looses itself in the secondary mylonitic material'. The Kishorn nappe is therefore a good area to study the changes in textures and fabrics with increase in Caledonian deformation.

This paper studies these changes using the following methods:
(i) by examining the change in shape of the clastic grains; (ii) by examining the change in textures as seen in thin section; (iii) by examining the magnetic anisotropy of the rock to see how this relates to bulk strain and to changes in shape and orientation of individual mineral

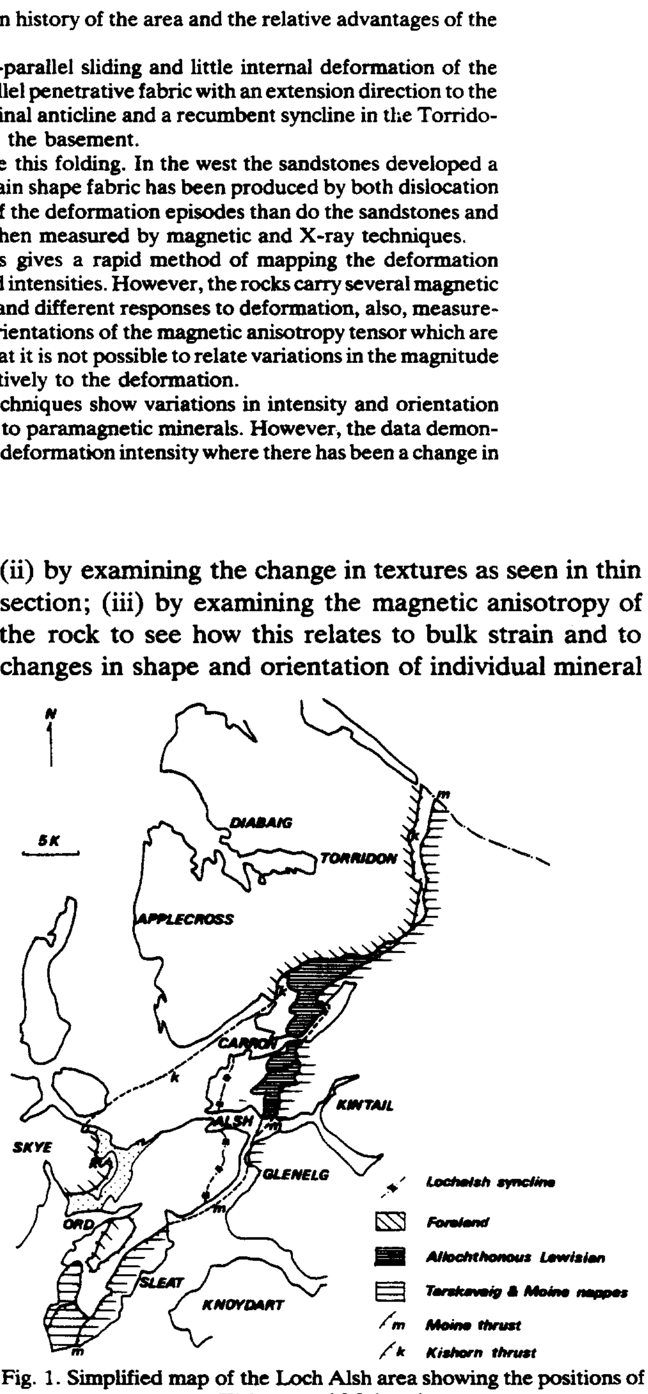

Fig. 1. Simplified map of the Loch Alsh area showing the positions of the Kishorn and Moine thrusts.

*Present address: Department of Geology, Portsmouth Polytechnic, Portsmouth, PO1 3QL, England.

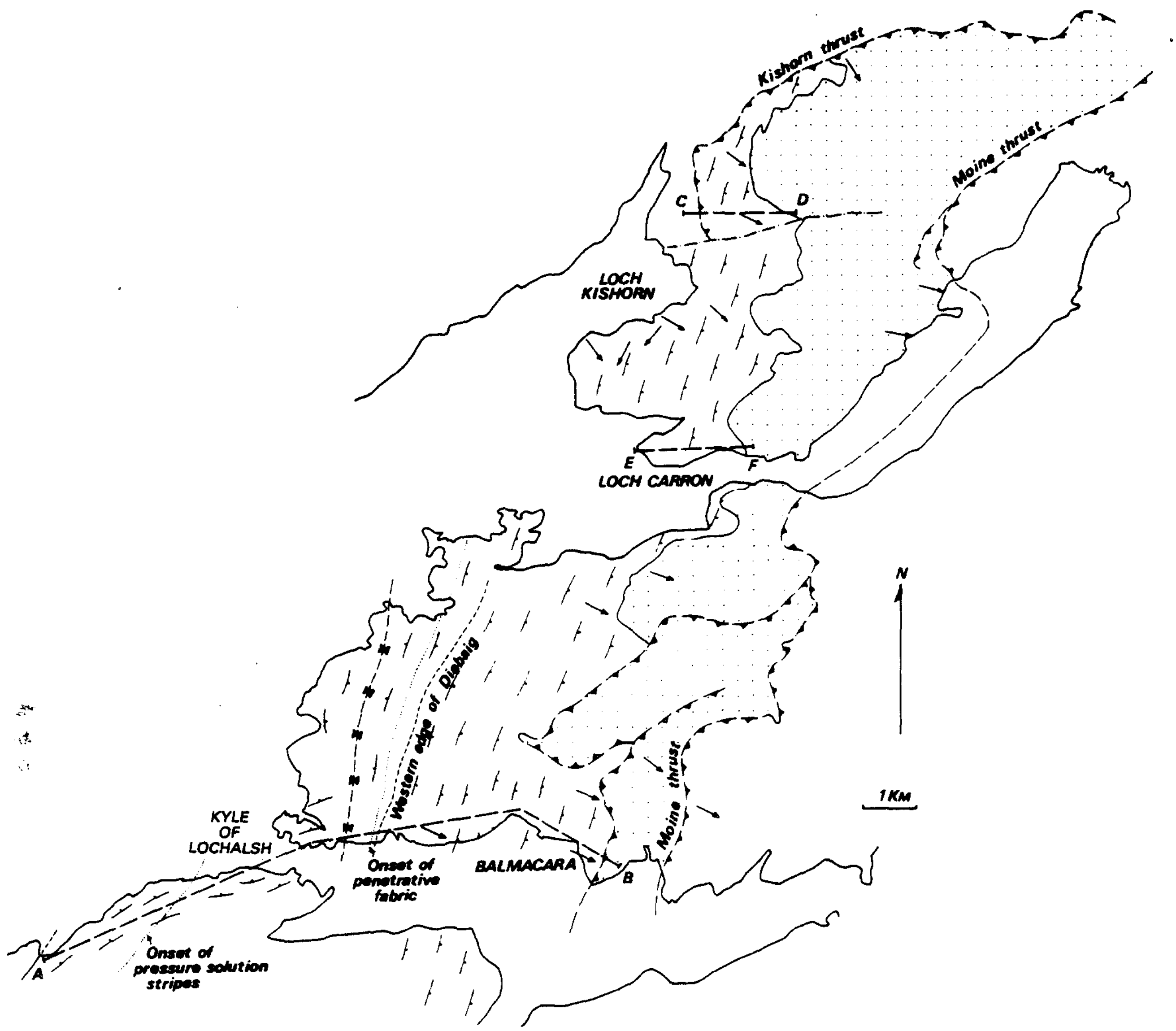

Fig. 2. Map of the Kishorn–Lochalsh area showing section lines AB, CD and EF, orientation of the bedding in the Torridonian and orientation of mineral lineation (arrows). The Lewisian is shown stippled.

phases; and (iv) by examining the change in preferred orientation of minerals, using an X-ray texture goniometer.

Samples have been examined from the northern part of the nappe, between Kishorn and Skye, with special emphasis on the section between Kyle and Balmacara, on the north shore of Lochalsh (Fig. 2).

STRATIGRAPHY AND STRUCTURE

The structure of the Kishorn nappe is one of Torridonian sandstones folded into a large recumbent syncline and thrust over Cambro-Ordovician rocks. The axial surface of the syncline passes through the village of Kyle of Lochalsh (Fig. 2). On Skye there is a complementary westward facing recumbent anticline (Bailey 1939, 1955). Torridonian stratigraphy has been described in detail by Peach *et al.* (1907). West of the axial trace of the Lochalsh syncline, along the flat, right-way up, fold limb, the massive sandstones and grits of the Applecross Formation crop out. East of the axial trace these rocks are structurally overlain but stratigraphically underlain by the Diabaig and Kinloch Formations. These are sandstones, flags and massive grits containing detrital microcline, oligoclase and quartz, similar to the Applecross Formation. East of the Kinloch Formation the massive sandstones and grits of the Ben na Seamraig Formation crop out, and east of Balmacara village these beds are overthrust by intensely deformed mylonites derived from Lewisian gneiss. At Loch Carron, to the north, the Ben na Seamraig Formation is stratigraphically underlain by shales and flags of the Loch na Dal Formation with layers of grit and conglomerate at the base. The inverted contact of these rocks with the Lewisian is probably the original unconformity, but it is now so intensely deformed that the original discordance has been obliterated.

The westernmost outcrops of the Applecross rocks in the Kishorn nappe show no cleavage, but near the Kishorn thrust plane they show some evidence of shattering and are considerably broken by quartz veins. To the east, near Kyle (Fig. 2) cleavage is shown by steeply dipping dark zones of pressure solution about 1mm wide and some 2–5mm apart.

Further to the east the cleavage becomes more intensely developed and penetrative in nature with a visible orientation of phyllosilicates in the finer grained lithologies. Cleavage in the sandstone layers maintains a spaced character but with visible flattening of quartz grains throughout the rock. There are small scale asymmetric folds with axial surfaces parallel to this cleavage.

To the east of Kyle of Lochalsh the dip of the bedding gradually decreases whilst the cleavage has a dip of 30–40° to the north-east, this being consistently a little steeper than the bedding throughout most of the section, and yet the beds are overturned. The cleavage must, therefore, post-date the folding and inversion of stratigraphy. The Kishorn thrust cuts across the Lochalsh fold and the zone of cleaved rocks and hence must post-date them.

Near Kyle of Lochalsh the bedding–cleavage intersection lineation plunges to the north-east but near Balmacara it plunges to the south-east and is often indistinguishable from a mineral lineation in the rock. This mineral lineation becomes more pronounced beneath the thrust, east of Balmacara and above the thrust plane there is a similar lineation in the mylonites. North of Loch Carron the lineation has the same south-east plunge, but near Kishorn Village it is more variable in orientation (Fig. 2) and locally plunges to the north-east or south-west.

Near Balmacara the cleavage and bedding are locally folded around upright structures which produce their own steeply dipping fracture cleavage. Similar late folds also occur in the Lower Torridonian rocks on either side of Loch Carron and in the mylonitised Lewisian rocks. Both bedding and foliation are folded by asymmetric and kink-band folds (Johnson 1960, Barber 1965). In the mylonites some of these folds are very tight and cause the development of a crenulation cleavage. The variations in morphology and orientation of these folds have been described by Barber (1965).

Between Kyle of Lochalsh and Balmacara there are numerous well-developed shear zones with en-echelon, sigmoidal veins infilled by quartz. There are two dominant orientations which constitute a conjugate pair. The set which shows a sinistral sense of shear dips at 50° to the north-west and the set with dextral shear dips at approximately 80° to the south-east.

THE CHANGE IN GRAIN SHAPE

The intensity of deformation is difficult to measure accurately due to a shortage of reliable strain markers in the Torridonian sandstones. Measurements have been made of the shape of deformed grains within the sandstones, but it is doubtful that these show the total deformation of the rock, especially at high strains. Also, the original grains become more difficult to identify towards the thrust zone. Measurements were made of the lengths of the long and short axes and of the orientations of the long axis for between 50 and 100 grains on each of three mutually perpendicular sections. The results were computed using the *Rf/Ø* method of Dunnet (1969) and the methods described by Dunnet & Siddans (1971). The results are summarised in Fig. 3. With increase in intensity of deformation to the east, the grains become more oblate. The maximum extension direction shown by these grains plunges gently to the east-south-east.

OPTICALLY DETERMINED TEXTURES

The sandstones and grits of the Applecross Formation in the west of the area show euhedral grains of quartz, microcline and oligoclase rimmed by fine grained material and a cement of quartz, sericite and calcite. Considering that these rocks have been thrust at least ten kilometres over the Cambrian rocks, as Cambrian rocks occur in the Ord window beneath the Torridonian rocks on Sleat (c.f. Bailey 1955), these sandstones show remarkably little deformation (Fig. 4a). The quartz grains show local strain shadows and undulose extinction and locally sub-grains have been produced. Where there is no intervening cement there has been pressure solution between the grains, the grain contacts being sutured and pitted and with undulose extinction near the pits. Within this area, west of Kyle, cleavage is only shown by dark stripes depleted in quartz.

East of Kyle, where the rocks are overturned, the quartz grains show a fabric (Fig. 4b). As there is no evidence of new quartz growth at the ends of the grains as seen in thin section, it is unlikely that the quartz grains changed shape by solution processes alone. The presence of undulose extinction and of sub-grains within original clastic grains is more common here and indicates the importance of intracrystalline, dislocation controlled deformation processes in this part of the traverse. In the east where the quartz grains are tabular, with micas parallel to the quartz grains there may have been considerable sliding along grain boundaries; the feldspar grains show fractures but no change in shape and must have deformed by fracturing and grain boundary sliding alone. East of Balmacara there are strings of opaque minerals, sphene and feldspar along the cleavage planes.

As the quartz grains show the development of sub-grains, with more intense deformation to the east, it becomes increasingly difficult to identify the original grains. Much of the quartz is in the form of sub-grains and new grains due to recovery and annealing processes (Fig. 4c).

In the east, below the Balmacara nappe, no original quartz grains remain; the only original sedimentary grains are strained and fractured feldspars (Fig. 4c). Some of the new quartz grains show exaggerated grain growth and there are small patches where all the quartz has recrystallised to form large new grains.

East of Kyle, the muscovite grains also show a preferred orientation. Muscovite grains form fibre-like growths in pressure shadows at the ends of the more competent feldspar grains, and also infill the necks of broken and boudinaged quartz and feldspar grains. They

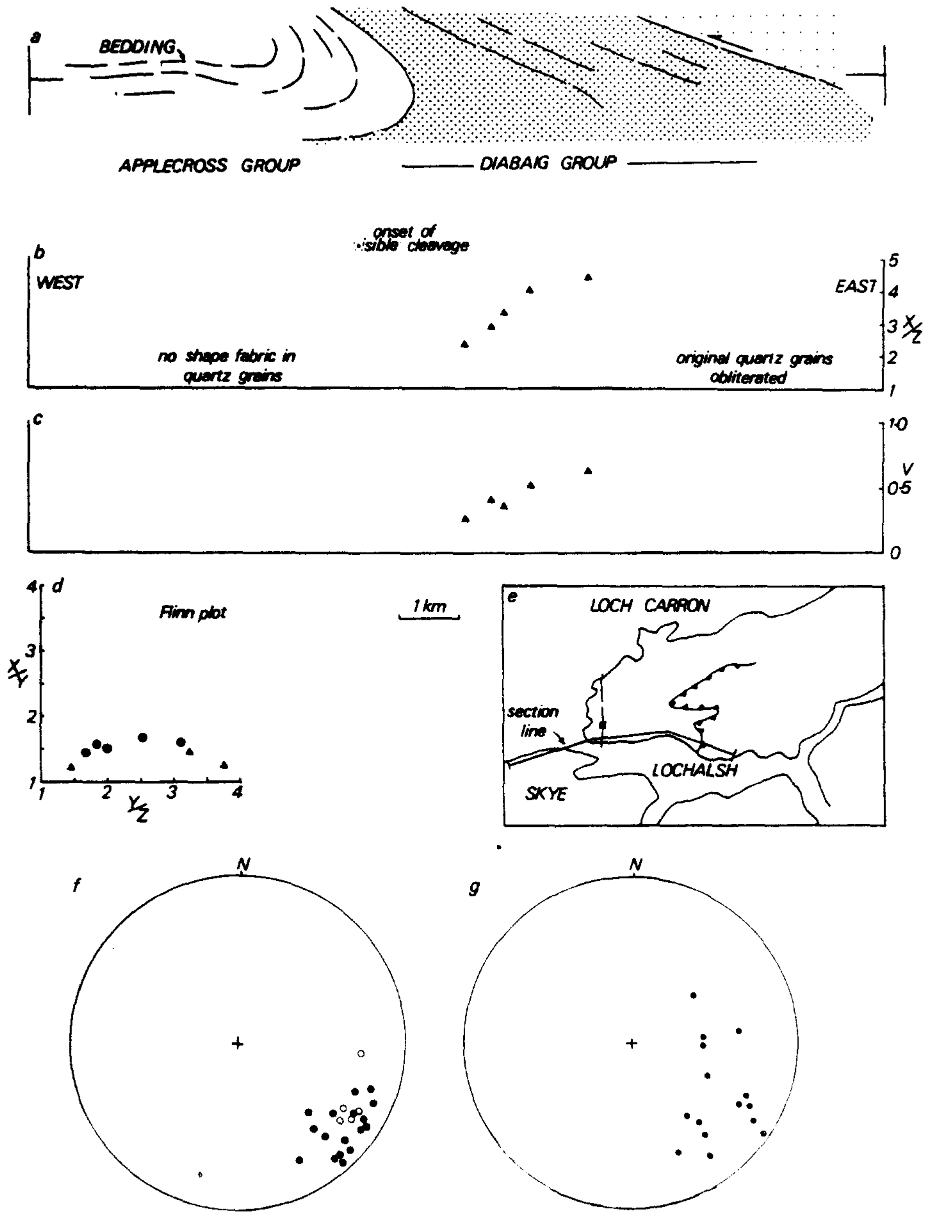

Fig. 3.(a) Simplified cross-section along AB in Fig. 2. (b) X/Z ratios of quartz grains along section AB. (c) Values of Lodes Unit (V) from shapes of quartz grains along section AB. For discussion of Lodes Unit see text, V is calculated from:

$$V = \frac{2\bar{Y} - (\bar{X} + \bar{Z})}{\bar{X} - \bar{Z}}$$

where $\bar{X}$, $\bar{Y}$ and $\bar{Z}$ are the natural strains along the principal axes of the strain ellipsoid. (d) Shapes of quartz grains plotted on a Flinn strain plot ($X > Y > Z$). The circles are ellipsoid ratios from section line AB, triangles are ellipsoid ratios from section line CD. (e) Locality map. (f) Lower hemisphere stereoplot of the mineral lineations for the Lochalsh section (closed circles) and the long axes of the measured grain shape fabrics (open circles). (g) Stereoplot showing the long axes of the susceptibility ellipsoids for the same section, for comparison. Measurements at low magnetic field.

coat and concentrate around the old quartz grains, but where deformation was more intense, they also coat some of the new grains within the boundaries of the old grains.

Muscovite and chlorite are most abundant within the quartz depleted pressure solution zones. The orientation of the long axes of the grains is usually sub-parallel to the edge of the zones. There is then, ample evidence of crystallisation of new mica during the cleavage producing deformation.

The shape fabric of the quartz grains as well as the preferred orientation of micas defines the macroscopic cleavage in the rocks. As noted before, this cleavage is oblique to the main Lochalsh fold. In some rocks, near Balmacara, it is possible to identify slightly elongate quartz grains which define an earlier fabric. These grains define a bedding parallel fabric which is deformed by folds with axial surfaces parallel to the main cleavage. Small scale folds of cleavage age also fold thin sheets of quartz fibres which lie parallel to bedding planes. These sheets are considered to represent slickensides associated with the main Lochalsh fold and support the proposition that folding took place by means of flexural slip with sliding taking place along bedding planes. The fibres plunge to the ESE.

Near Balmacara there is also a late fabric defined by

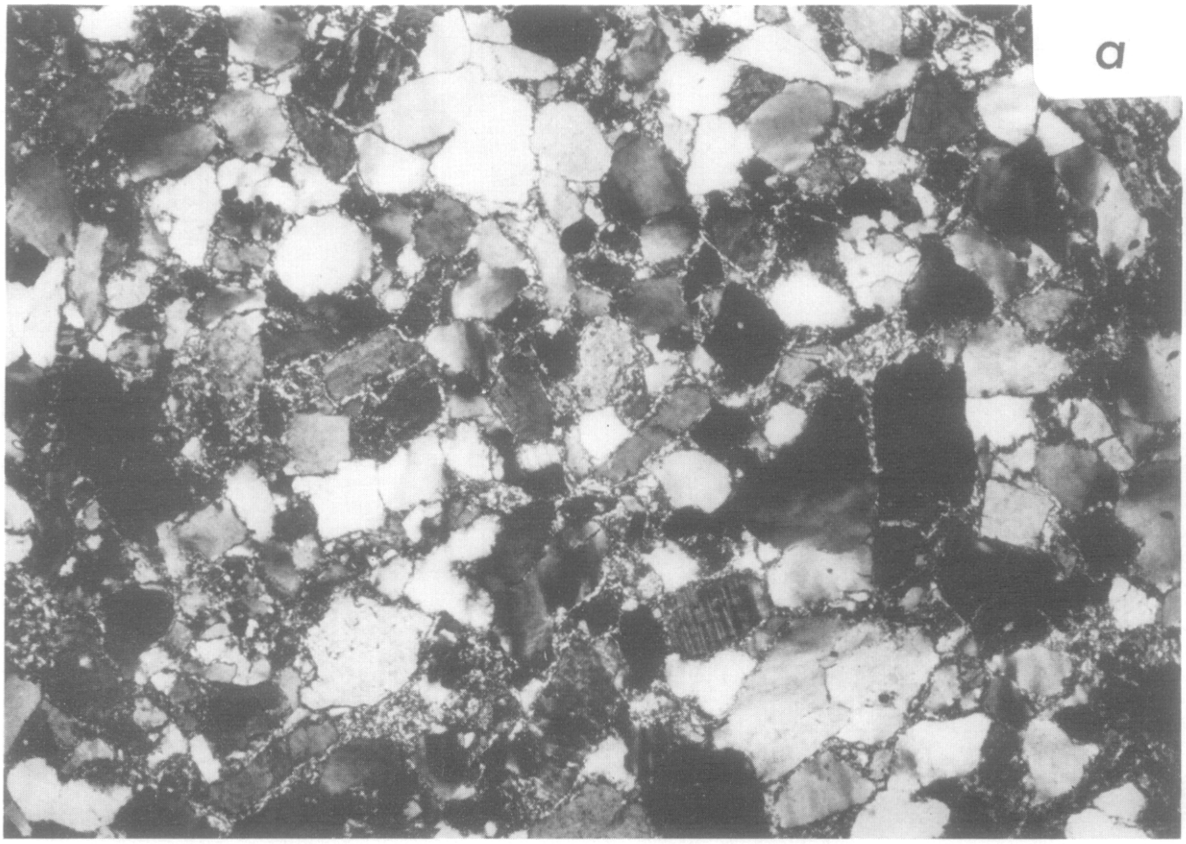

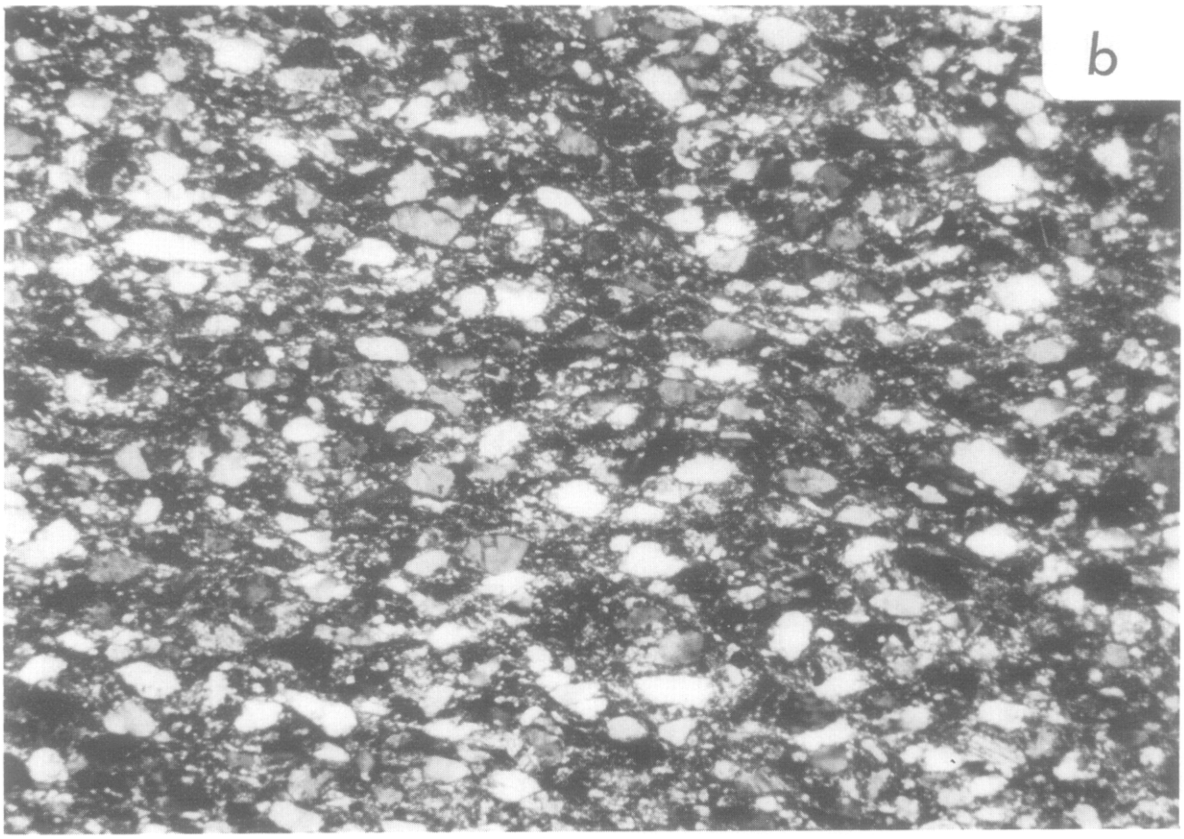

Figs 4 (a) and (b) captions on p. 264.

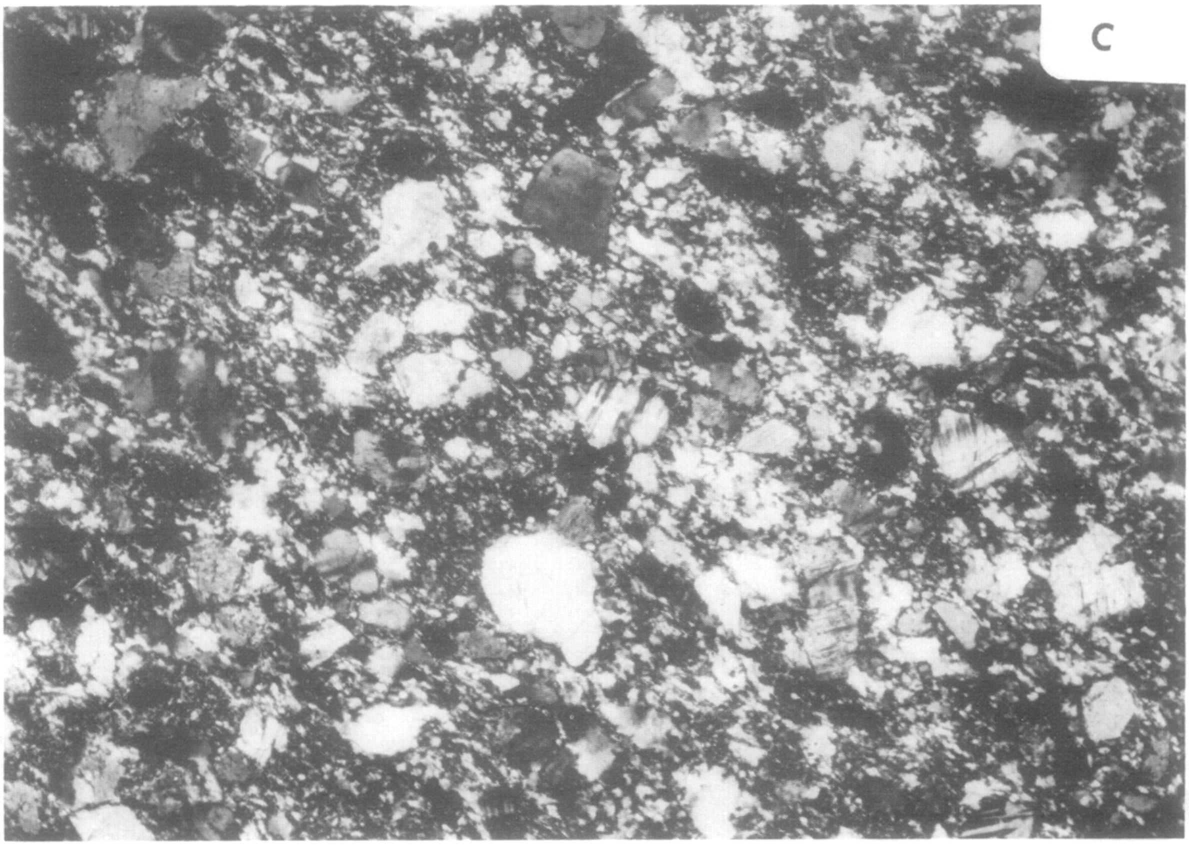

Fig. 4. Photomicrographs of Torridonian sandstones. (a) is from locality 3 (Fig. 10) from the overturned limb of the Lochalsh fold. The quartz grains show sutured margins and undulose extinction. Small sub-grains have formed round the margins. (b) is from locality 5 (Fig. 10) where the rock shows a visible cleavage. The quartz grains show a fabric and the development of sub grains. (c) is from locality 7 (Fig. 10) near the thrust. Most of the original quartz grains have been broken down to sub grains. The large crystals are of feldspar. The width of the field shown on the photograph is 30mm.

Table 1. Structures and textures in the Torridonian rocks of the Kishorn Nappe

Deformation event	Structure	Textures: Western area	Textures: Eastern area	Comments
D_1	Lochalsh syncline, and anticline at Ord on Skye Decoupling of Torridonian and Lewisian rocks on Skye	Bedding parallel slip giving slickensides	Bedding parallel slip and localised bedding parallel penetrative fabric. Extension direction to the ESE. Possibly shearing of the Lewisian rocks associated with inversion of eastern limb of Lochalsh fold	Grain shape fabric detected by magnetic methods in the sandstones. In the shales this fabric may be overprinted by D_3
D_2	Folding of bedding and slickensides	Pressure solution cleavage and grain shape fabric in the east – dipping more steeply than bedding. Grain shape fabric is a finite fabric as a result of D_1 and D_2		Dominates the magnetic and X-ray fabrics in the shales
D_3	?Shearing of inverted limb of Lochalsh fold		Bedding parallel fabric cutting existing folds. Intensification of earlier fabrics and structures	
D_4	Upright open folds and later kink band folds Tension gash shear zones Final emplacement of Kishorn Nappe		Local fracture and crenulation cleavages	

elongate quartz grains and micas which, whilst it is usually parallel to bedding, in fact cuts across small folds which have axial surfaces parallel to the main cleavage. Thus there was a complex history of cleavage production.

THE MAGNETIC FABRIC

Measurement and representation

The magnetic fabric was measured at low magnetic fields using a modification of the spinner magnetometer (Molyneux 1971) in the School of Physics University of Newcastle-upon-Tyne, and at high fields using the high field torque magnetometer (Stacey 1960) at the Department of Earth Sciences, University of Leeds.

Shape anisotropy (Stacey 1960) is caused by the shape alignment of ferromagnetic grains, magnetite or titanomagnetite. The anisotropy is measured in a high, saturating magnetic field where the torque, T, is given by

$$T = \tfrac{1}{4} v J_s^2 \, (N_b - N_a) \sin 2\emptyset$$

where v is the volume of the sample, J_s the saturation magnetisation, N_a and N_b the demagnetising factors along two orthogonal principal axes, N_a making an angle $\emptyset$ with the field direction.

At low fields for rocks containing ferromagnetic minerals and at any fields in paramagnetic rocks, the induced magnetisation, J, is given by

$$J = \bar{k}H$$

where $\bar{k}$ is the apparent susceptibility at the field H. In anisotropic rocks, $\bar{k}$ is a second order tensor which can be represented by an ellipsoid with the three principal axes k_1', k_2', and k_3': In this paper,

$$k_1' \geqslant k_2' \geqslant k_3'.$$

These principal axes are represented diagramatically as natural logarithmic values on the octahedral plane (c.f. Nadai 1963, Hsu 1966) of the anisotropy ellipsoid, a plot similar to that described by Owens (1974) for natural strain. The intensity or magnitude of anisotropy, H_s, is the distance from the origin on the diagram and can be calculated from

$$H_s = \tfrac{2}{3} \, [(k_1 - k_2)^2 + (k_2 - k_3)^2 + (k_3 - k_1)^2]^{\frac{1}{2}}$$

where $k_1 = \log_e (k_1'/k)$ etc., k being the bulk susceptibility. The symmetry of the anisotropy ellipsoid is described by a parameter V, similar to Lode's unit in strain analysis (Hossack 1968), where

$$V = \frac{2k_2 - (k_1 + k_3)}{k_1 - k_3}$$

This parameter has the advantage that it is symmetrical about the plane anisotropy ellipsoid, $V = 0$, with $V = +1$ for a uniaxial oblate ellipsoid and $V = -1$ for a uniaxial prolate ellipsoid.

Identification of magnetic minerals

The Torridonian rocks contain a range of magnetic minerals. Magnetite occurs as heavy detrital grains, often elongated along the bedding surfaces in the undeformed Applecross beds. There are occasional large grains of magnetite in the Ben na Seamraig grits. Hematite occurs as large irregular masses and also coats the grains in the grits of the Applecross beds. Chlorites and micas are prominent in the flaggy sediments and to a lesser extent in the sandstones, whilst in the more deformed rocks, new, metamorphic muscovite grains have crystallised. In order to identify the main magnetic phase in each particular rock, measurements were made of the torque T, and rotational hysteresis W_R, at different fields H (c.f. Day *et al.* 1970).

Specimens from the Applecross beds, west of Kyle,

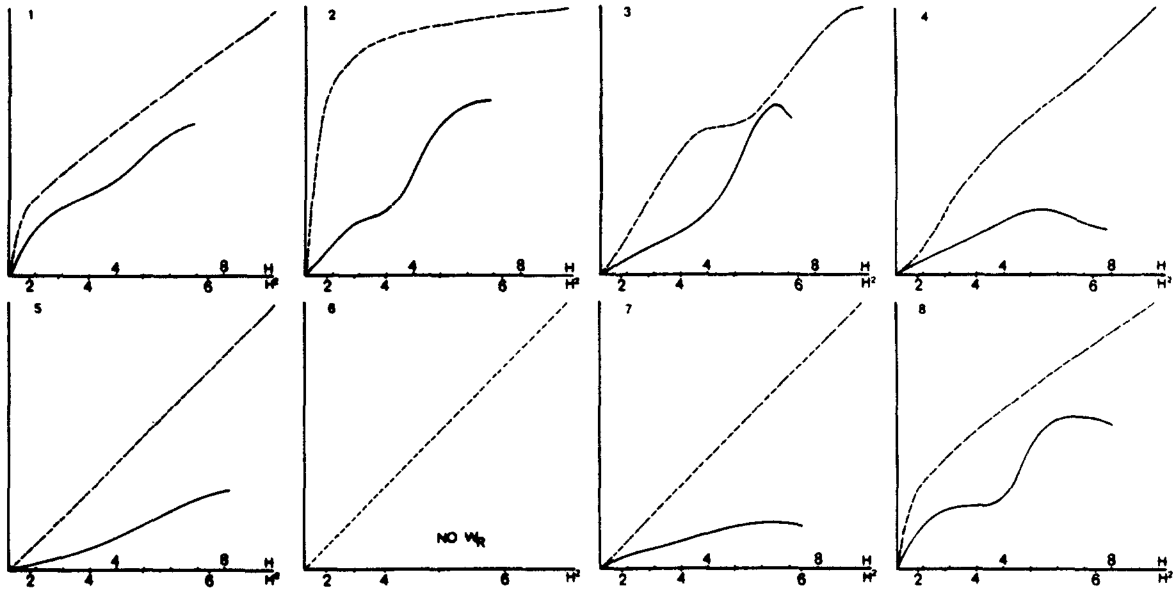

Fig. 5. Plots of torque against field squared (H^2) dashed lines, and rotational hysteresis (W_R) against field (H) solid lines. Torque values standardised to a percentage of T_{max}, the torque at the maximum measured field strength of 6.8 kOe. W_R values here are dimensionless. W_R was obtained from torque curves plotted as the field was rotated from 0 to 360° and 360° to 0°, the area enclosed by the curves is a measure of the work done during two cycles and is proportional to the rotational hysteresis (see Day *et al.* 1970, for details). Specimen locations shown in Fig. 10, details given in the Appendix.

show a component of saturation magnetisation at relatively low fields, but generally there is a very complex T/H^2 relationship due to the presence of hematite as well as magnetite (Fig. 5). This is supported by plots of W_R/H which show a peak at low field values, generally with a second peak at high fields (Fig. 5).

Specimens from the sandstones and many of the shales east of Kyle, show T/H^2 curves which do not saturate and hysteresis curves which increase with field (Fig. 5), probably indicating the dominance of hematite over other magnetic minerals. Specimens from certain sandstones of the Ben na Seamraig grits however, show T/H^2 curves which have a well defined elbow at low field values and then a steady, linear T/H^2 relationship at higher fields (Fig. 5). These suggest the presence of a saturating component, probably magnetite, as well as the hematite and/or paramagnetic minerals.

Many of the flags and shales within the Kinloch beds and Ben na Seamraig grits appear paramagnetic; there is no rotational hysteresis and the T/H^2 curves are purely linear (Fig. 5). The magnetic properties of these flaggy rocks are due to paramagnetic minerals such as chlorites and micas.

The magnetic minerals have thus been separated into three groups for the purposes of this paper; a saturating group comprising the ferromagnetic minerals which saturate at low fields, the hematite group and a linear group which include almost all the other minerals in the rock. The linear group show a steady T/H^2 relationship at the measured fields. Hematite should have a linear T/H^2 relationship and is often indistinguishable from paramagnetic minerals at these fields. However, it may be identified separately from the other members of the linear group due to its hysteresis.

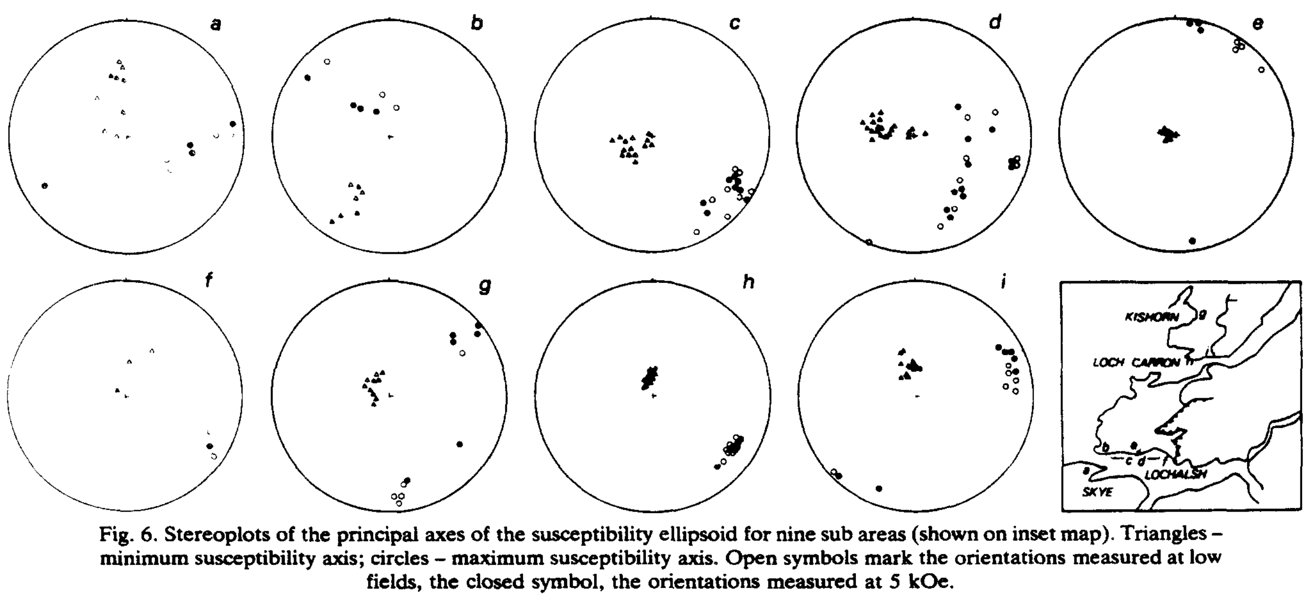

Fig. 6. Stereoplots of the principal axes of the susceptibility ellipsoid for nine sub areas (shown on inset map). Triangles – minimum susceptibility axis; circles – maximum susceptibility axis. Open symbols mark the orientations measured at low fields, the closed symbol, the orientations measured at 5 kOe.

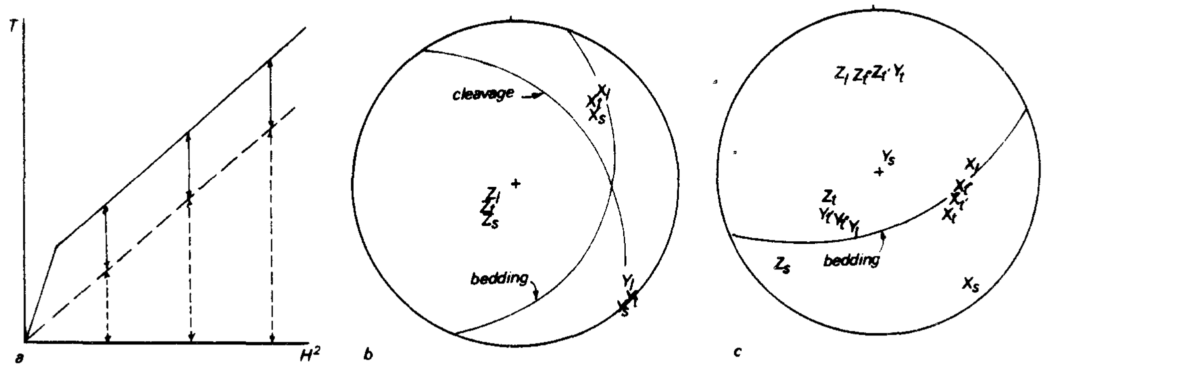

Fig. 7(a). Torque curve (torque against field squared) for a specimen containing a saturating and a linear component. From the curve the saturating component can be measured (solid vertical line) and the linear component (dashed vertical line) are various fields. (b). and (c). The orientation of the principal axes of susceptibility in specimen 8 (Fig. 6b) and 1 (Fig. 6c). The locations of specimens are shown in Fig. 9. X – maximum susceptibility; Y – intermediate; Z – minimum; S – saturating component; L – Linear component; t, t', t'', bulk susceptibility ellipsoids at increasing fields, $t = 2.25$ kOe, $t' = 5$ kOe, $t'' =$ 6.3 kOe.

The orientation of the principal axes

The direction of k_1, the maximum axis and k_3, the minimum axis of the magnetic fabric ellipsoid, are plotted in Fig. 6. East of Kyle the k_3 direction in the shales lies close to the pole to bedding, but in the coarser units it lies nearly parallel to the pole to cleavage (Figs. 6c and d). In the shaly beds the k_1 direction shows a spread of orientations within the bedding planes, but in the coarser rocks, k_1 is parallel to the direction of maximum mineral elongation. The sandstone layers show k_1 in this orientation as far west as Kyle, where no mineral lineation is visible in the hand specimen.

An attempt has been made to separate the different magnetic components, to examine in more detail the bedding plane and cleavage plane fabrics. Figure 5 shows how some sandstones contain both saturating magnetic components and also another component which gives a linear T/H^2 curve. Measurements of torque were made at a wide range of fields and the curves plotted as in Fig. 7(a). This enabled separation of the torques due to the saturating and linear components.

Specimen 1, from the right way up beds at Kyle shows different orientations for the saturating and linear components (Fig. 7c). The k_1 and k_2 directions of the linear component lie within the bedding plane, but the $k_1 - k_2$ plane of the saturating component lies normal to the bedding and the k_1 direction approximates to the direction taken by the mineral lineation in the more deformed rocks east of Kyle. Neither the $k_1 - k_2$ plane of the saturating component nor of the linear component lies close to the plane of the pressure solution stripes. Thus we can conclude that the flaky minerals which make up the linear magnetic component lie within the only visible foliation plane in the rocks, that is the bedding plane, whilst the magnetite grains have a shape fabric which is highly oblique to bedding, but which cannot definitely be related to any tectonic fabric.

Specimen 8 from the more highly deformed sandstones on the south shores of Loch Kishorn shows saturating and linear components with nearly parallel principal axes. In these more deformed rocks, the elongation direction of the magnetite grains is parallel to the mean orientation of the paramagnetic grains.

Figure 7(a) shows that as the torque is measured at increasingly higher fields, the torque due to the linear magnetic component becomes more important than the torque due to the saturating component. This is also shown in Fig. 7(c) where the measured paths of the principal axes are plotted, X_s being the k_1 direction of the saturating component, X_L the k_1 direction of the linear component and X_t, K_t', X_t', the k_1 direction at increasingly higher fields. This path is formed by the addition of an increasing fraction of the linear anisotropy tensor to a constant saturating anisotropy tensor.

At the fields used during this work, both on the low field spinner magnetometer and on the high field torque magnetometer, it is the linear component which dominates the total magnetic tensor, but measurements on the high field torque magnetometer record far more of this linear component, than do the measurements on the low field magnetometer. Thus it is to be expected that the anisotropy values will be different when measured at different fields and the orientation of the principal axes will be different, as shown in Fig. 6.

For each specimen studied the k_1 direction measured at low fields makes an angle θ with the k_1 direction measured at 5 kOe, and always lies closer to the mineral lineation in the rock. From Kyle to the thrust at Balmacara, the k_1 directions measured at low and high fields approach this direction of mineral lineation, and the angle θ decreases (Fig. 8). This suggests an eastward

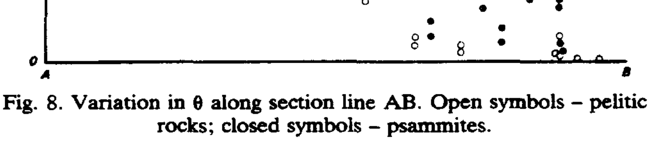

Fig. 8. Variation in θ along section line AB. Open symbols – pelitic rocks; closed symbols – psammites.

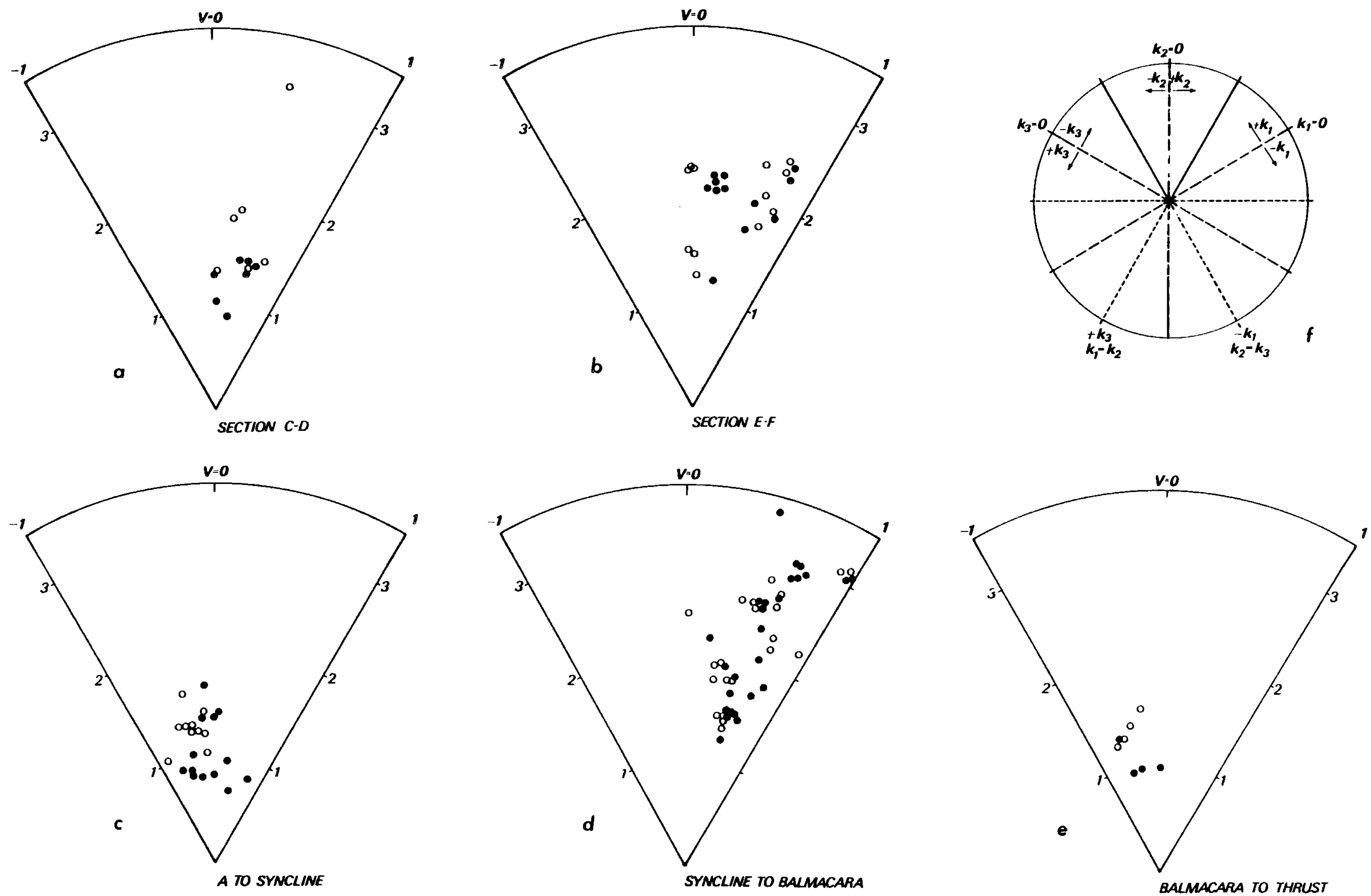

Fig. 9. Intensities of anisotropy at high field (5 kOe), plotted on the octahedral plane. Closed circles – psammites; open circles – pelites. (f) shows the octahedral plane with solid lines outlining the segment used in (a) to (e).

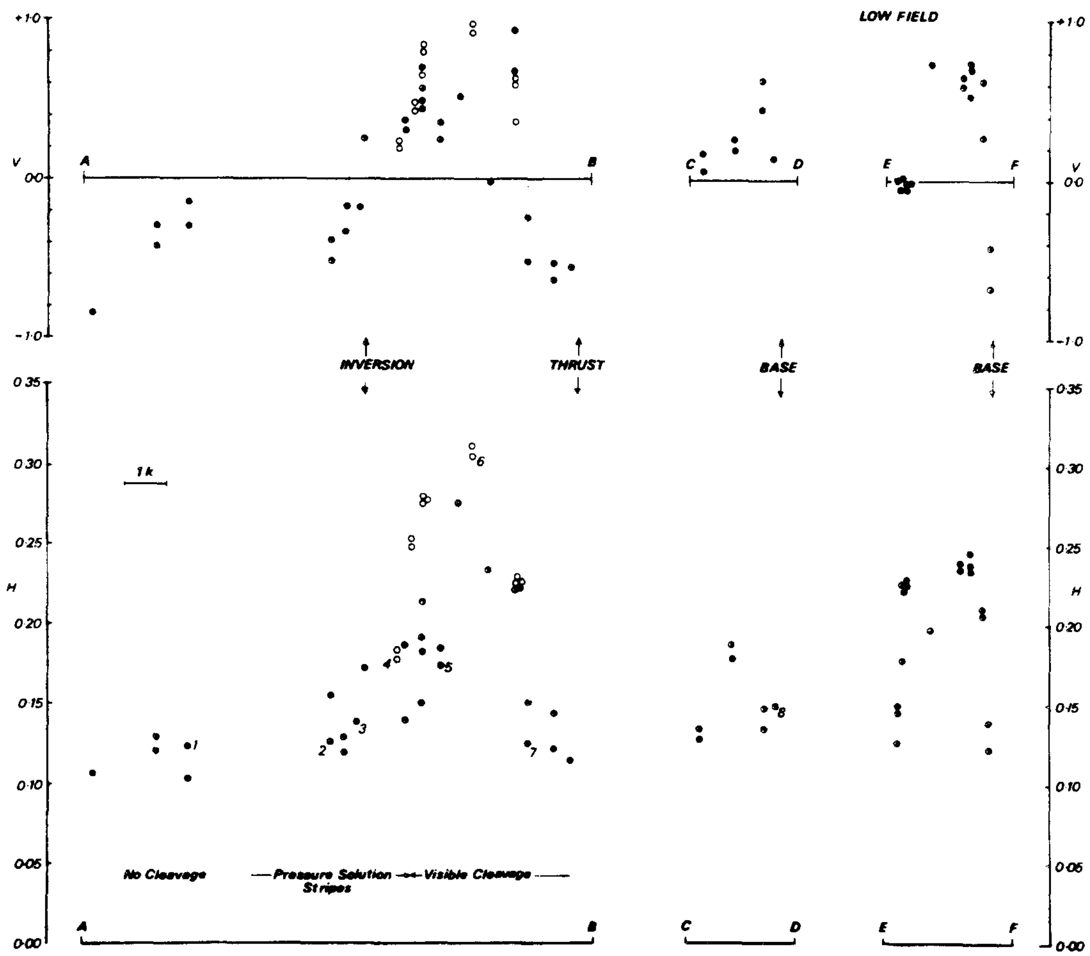

Fig. 10. Intensities of anisotropy (H_S) measured at low fields, plotted along section lines AB, CD and EF and values of V plotted along the same lines. Closed symbols – psammites; open symbols – pelites. The intensities of anisotropy measured at high fields give a similar plot and this can be provided by the authors on request.

increase in colinearity of the magnetic fabric ellipsoids for the saturating and linear components.

The intensity of the magnetic anisotropy

The intensities of the anisotropy of magnetic fabric are plotted on the octahedral plane of the anisotropy ellipsoid in Fig. 9, in a section across the Lochalsh fold in Fig. 10 and in map form in Figs. 11(a) and (b). Measurements at both high and low fields show a similar change in anisotropy across the fold, though the high field measurements give more oblate ellipsoids, presumably due to the higher fraction of paramagnetic minerals or hematites making up the total anisotropy. These hematites and paramagnetic minerals are themselves oblate flakes, and Owens (1974b) has shown how a plane strain distribution of particles with individual oblate anisotropy can give an oblate total magnetic anisotropy to the rock.

West of Kyle the total anisotropy ellipsoid is prolate, but this may be a combination of the two anisotropy tensors. Figure 7 shows that as the fraction of the anisotropy due to linear magnetic component increases relative to that of the saturating component, the k_2 axis becomes the k_3 axis and the k_3 axis becomes the k_2 axis. In specimen 2 (Fig. 7), this changeover takes place at fields between 2 and 3 kOe. Thus in both the low field and high field measurements, k_2 is similar in value to k_3 and the resultant anisotropy is prolate. No evidence has been detected for a prolate mineral fabric in the rock; there is no detectable sedimentary or tectonic lineation in this area.

Immediately east of Kyle the anisotropy increases in intensity and the susceptibility anisotropy (measured at low fields) is greater than the anisotropy of Js (measured at high fields). As expected, the shaly or flaggy beds show a more intense and more oblate anisotropy than the massive sandstone units. This trend matches that shown by the increasingly oblate quartz grains in this section (see Figs. 3 and 10).

The decrease in intensity of anisotropy near the thrust plane and the change to prolate anisotropy must mark some change in the deformation processes operating in the rock. Flaky minerals such as chlorite and mica are unlikely to give a prolate anisotropy to the rock unless their distribution is markedly prolate (Owens 1974b). The directions of the principal axes of the saturating and linear components are nearly parallel in this zone. The k_1 direction is identical at high and low fields, and so the prolate anisotropy cannot be due to the two groups of magnetic minerals having differently orientated anisotropy ellipsoids. The anisotropy decreases and becomes prolate at the point where the original grains in the rock cease to be identifiable. It is suggested that within this

Fig. 11(a). Map showing variation in intensity of anisotropy. Shaded area intensity (H_S) greater than 0.20. (b). Map showing variation in oblateness of anisotropy ellipsoid. Heavy stipple, V less than 0.0 (i.e. prolate), blank, V between 0.0 and 0.4, horizontal shading, V greater than 0.4. Maps drawn from sections AB, CD and EF and individual anisotropy measurements (solid circles) south of Loch Carron. These m:ps include several geological assumptions, such as that variations in oblateness or in intensity of magnetic anisotropy are parallel to the main structural trends.

zone there is another mechanism of deformation, probably one of grain boundary sliding and rotation of the sub-grains and new grains of quartz and hence also the muscovite and hematite which wrap around these grains. This zone is also one of exaggerated new grain growth of both quartz and muscovite. Thus within this zone, the anisotropy due to the preferred orientation of the hematites and the paramagnetic flaky minerals may be expected to decrease. The cause of the prolate anisotropy is unknown.

This change in deformation mechanism is presumably associated with shear and sliding along cleavage planes. Such movement must also have taken place at the base of the Torridonian succession, adjacent to the Lewisian rocks, north of Loch Carron, as these rocks show a similar decrease in intensity and anisotropy.

X-RAY TEXTURE MEASUREMENTS

Measurement techniques

The orientation distributions of poles to basal planes of muscovite and chlorite were measured using a McLeans X-ray texture goniometer. The pole figures of these distributions were determined using the combined reflection/transmission mode techniques described by Siddans (1976). In order to provide direct compatibility from specimen to specimen, the intensity data are expressed in terms of normalised units (Siddans 1976). A pole density of one normalised unit is the pole density expected in every direction from a random distribution of poles. The units are consequently referred to as 'times random'.

Two parameters have been chosen to describe these fabrics. The maximum pole density, expressed in normalised units, provides a measure of the intensity of fabric development. The second moment of the distribution about the direction of the maximum pole density gives a measure of the tightness of the distribution. A second moment value of 1.0 would represent a perfect point maximum.

As a preliminary to making the texture measurements a $\theta/2\theta$ diffraction scan was made of each sample. Muscovite and chlorite diffraction peaks were identified in all of the fine grained samples and most of the sandstones. Measurements of the 10Å peak width at half peak height were made in order to gain an estimate of the Kubler Index (Kubler 1968) of the degree of ordering of the muscovite/illite lattice. These measurements showed that all the samples contained metamorphic muscovite and there was no detectable non-metamorphic illite even in the most western samples.

Results of the X-ray measurements

Figures 12(a) and (b) show the variations of the two

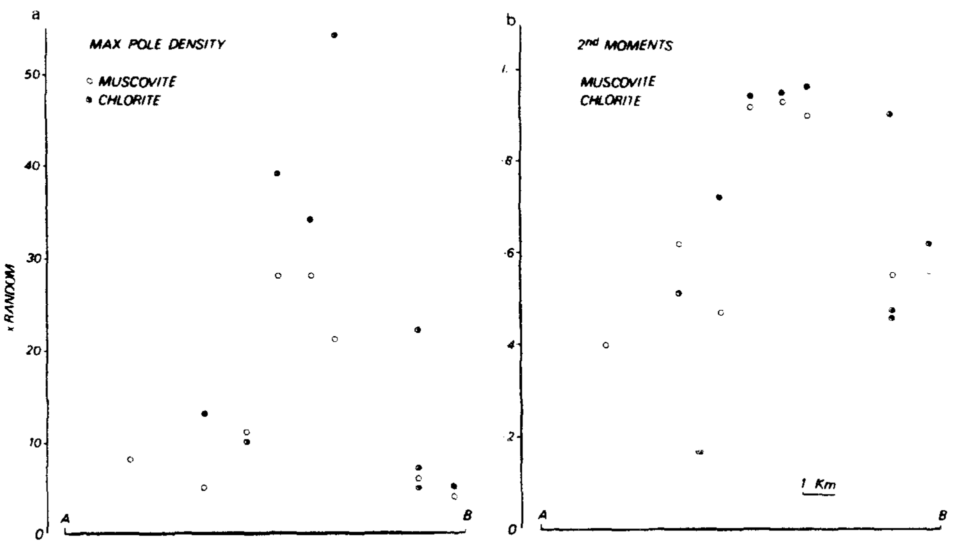

Fig. 12(a) Variation in maximum pole density along section line AB (Fig. 2) for basal planes of muscovite and chlorite. (b) Variation in second moment along line AB. Solid circle, chlorite; open circle, muscovite.

parameters, maximum pole density and second moment, along the section line AB, for both muscovite and chlorite basal planes. The fabric, as defined by the phyllosilicate grains, increases in intensity from west to east and reaches a maximum in the area of visible cleavage. There is a reduction in intensity in the area immediately beneath the thrust.

The orientation data for specimen 4 are shown in Fig. 13(a). Cleavage in this sample is visible at a high angle to the bedding but the poles to both sets of basal planes cluster around the pole to bedding. There is no measureable concentration of poles around the pole to cleavage. In specimen 6 (Fig. 13b) there is a much smaller angle between the pole to bedding and the pole to cleavage, but there is still a grouping of the poles to basal planes of phyllosilicates about the pole to bedding. These data are illustrative of a general relationship; the maximum pole densities of muscovite and chlorite fabrics plot closer to the pole to the visible bedding, or bedding-parallel fabric, rather than to any other visible fabric in the rock.

Discussion of X-ray texture measurements

The variations in intensity of fabric as revealed by the X-ray measurements broadly agree with those detected by magnetic means. However, it is clear from previous discussions regarding the complex make-up of the anisotropy components and the fact that these rocks carry more than one fabric that any attempt to make a detailed numerical correlation between them would be futile.

DISCUSSION

The history of the Lochalsh fold involves several phases of deformation, cleavage development and recrystallisation, and is summarised in Table 1. The sequence correlates with Barber's (1965) structural sequence; the D_1 phase correlates with Barber's phase of mylonitisation above the Kishorn Nappe, the D_2 phase correlates with Barber's phase of asymmetric folds.

It is evident that the early deformation was well lubricated, with layer parallel sliding and little internal deformation of the rocks, though an early bedding-parallel fabric has been detected from near Balmacara. Folding was accommodated with only locally developed penetrative fabrics but with the development of quartz fibres along bedding planes. Outside the present area, near Ord on Skye (Fig. 1), there is a recumbent isoclinal westward facing antiform probably the same age as the

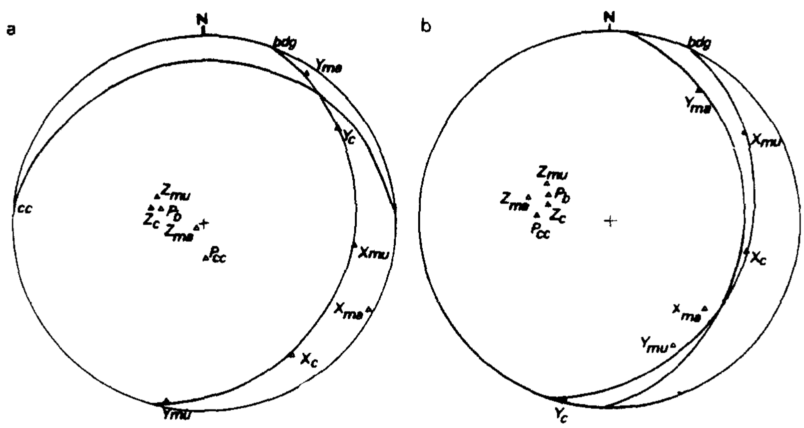

Fig. 13. Stereographic projection of the three fabric axes (X>Y>Z) for muscovite (mu), chlorite (c) and the magnetic anisotropy (ma) for specimens 4 (a) and 6 (b). bdg = bedding, P_b = pole to bedding, cc = cleavage, P_c = pole to cleavage. The field strength for the magnetic anisotropy measurements was 5 kOe.

Lochalsh fold, and here also, there is little internal deformation. Near Kyle and on Skye the rocks show no penetrative cleavage associated with the folding. It is not known how this early, tight deformation has affected the basement. The Lewisian rocks east of the Lochalsh fold are highly sheared and some of this shearing may be associated with the inversion of the eastern limb of the Lochalsh fold, the tight cleavage-free antiform to the west, at Ord, suggests a decoupling of the basement and cover rocks during this phase. Quartz fibres plunge to the south-east, suggesting tectonic transport from this direction though the fibres may also have formed by layer parallel slip, due to flexural shear normal to the hinge of the Lochalsh fold. The penetrative grain elongation which also plunges to the east-south-east may be a result of the D_1 and D_2 phases, though Barber (1965) records D_2 folds which fold an earlier ESE plunging lineation.

Subsequent deformations (D_2 to D_3) took place under higher temperatures, as is evident from the metamorphic muscovite and lack of original, detrital clay minerals. The high temperatures allowed diffusion and dislocation processes to operate. The deformation was restricted, and commonly localised along the shales rather than the sandstones. The shales show more deformation episodes, more intense deformation and more metamorphic crystallisation than do the sandstones. Thus the shales show fabric intensities and orientations which are different from those shown by the sandstones when measured by magnetic and X-ray techniques.

East of Lochalsh, the main D_2 cleavage/bedding intersection plunges towards the SE suggesting localised shortening of the thrust zone normal to the strike of the thrust. The significance of this localised shortening will be discussed in a separate paper (Coward & Kim, in press). A late bedding-parallel fabric (D_3) occurs in the east.

The rocks carry a complex mineralogy with several magnetic components which have different anisotropy tensors and different responses to deformation. Many sandstones contain several components together. Thus it is not possible to relate variations in the intensity of magnetic anisotropy and shape of the anisotropy ellipsoid directly to the deformation. This conclusion is in contrast to that of Wood *et al.* (1976) who showed a quantitative correlation between the magnitude of the axes of the magnetic susceptibility ellipsoid and those of the deformation ellipsoid. However, in the area studied by Wood *et al.* (1976) in North Wales, the deformation sequence was simpler and the rocks contained hematite as the only magnetic component.

The magnetic anisotropy technique of fabric analysis has given a rapid method of mapping the different deformation domains formed by differing deformation mechanisms and intensities (Fig. 11). It has shown where the fabric is most intense and where textures produced by diffusion and dislocation processes are partly obliterated by rotation and grain boundary sliding.

The phyllosilicate fabric measured by the magnetic and X-ray method is parallel to bedding. It is taken to be a combination of the different fabrics formed during the deformation sequence, but largely that fabric termed D_3 in Table 1. This is a later fabric than that still recorded by the sandstones. Neither the magnetic nor X-ray techniques measure quantities which can be numerically related to strain, and the problems associated with attempting such correlation for rocks in which a simple combination of deformation mechanisms has operated have been discussed by Siddans (1976) and Owens & Bamford (1976). The data presented in this paper particularly illustrate the difficulty of correlation when a change in deformation mechanisms with time and space can be demonstrated. The most intensely deformed rocks, near the thrust, show less than the maximum intensity of fabric.

The X-ray technique does not have the advantage of the speed of determination of the magnetic technique but that can sometimes be outweighed by the fact that the fabric determined by the X-ray technique is known to be that due to just one mineral.

Acknowledgements—This work was carried out whilst one of us (J.S.W.) held a Natural Environment Research Council Studentship, which is gratefully acknowledged. We would like to thank Dr. L. Molyneaux of the School of Physics, University of Newcastle-upon-Tyne for allowing us to use the magnetic anisotropy spinner in that department. We have benefited from discussions with Dr. A. J. Barber, Dr. W. Owens, Dr. A. W. Siddans and Dr. L. I. Wright to whom we extend our thanks.

REFERENCES

Bailey, E. B. 1939. Caledonian tectonics and metamorphism in Skye. *Bull. geol. Surv. G.B.* **2**, 46–62.

Bailey, E. B. 1955. Moine tectonics and metamorphism in Skye. *Trans. Edinb. geol. Soc.* **16**, 93–166.

Barber, A. J. 1965. The history of the Moine Thrust zone, Lochcarron and Lochalsh, Scotland. *Proc. Geol. Ass.* **76**, 215–242.

Coward, M. P. & Kim, J. H. in press. Strain within thrust sheets. In: *Thrust and Nappe tectonics.* (edited by McClay, K. and Price, N. J.) *Geol. Soc. Lond. Spec. Publ.*

Day, R., O'Reilly, W. & Bannerjee, S. K. 1970. Rotational hysteresis study of oxidised basalts. *J. geophys. Res.* **75**, 375–386.

Dunnet, D. 1969. A technique of finite-strain analysis using elliptical particles. *Tectonophysics* **7**, 117–136.

Dunnet, D. & Siddans, A. W. B. 1971. Non-random sedimentary fabrics and their modification by strain. *Tectonophysics* **12**, 307–325.

Hossack, J. R. 1968. Pebble deformation and thrusting in the Bygdin area (southern Norway). *Tectonophysics* **5**, 315–339.

Hsu, T. C. 1966. The characteristics of coaxial and non-coaxial strain paths. *J. Strain. Anal.* **1**, 216–222.

Johnson, M. R. W. 1960. The structural history of the Moine thrust zone at Lochcarron, Wester Ross. *Trans. R. Soc. Edinb.* **64**, 139–168.

Kanungo, D. 1956. The structural geology of the Torridonian, Lewisian and Moinian rocks of the area between Plockton and Kyle of Lochalsh in Wester Ross, Scotland. Unpublished Ph.D. thesis, University of London.

Kubler, B. 1968. Evaluation quantitative du métamorphisme par la cristallinité de l'Illite. *Bull. Centre Rech. Pau — S.N.P.A.* **7**, 385–397.

Molyneux, L. 1971. A complete result magnetometer for measuring the remanent magnetism of rocks. *Geophys. J. R. astr. Soc.* **24**, 429–433.

Nadai, A. 1963. *Theory of Flow and Fracture of Solids.* McGraw-Hill, New York.

Owens, W. H. 1974a. Representation of finite strain state by three axis planar diagrams. *Bull. geol. Soc. Am.* **85**, 307–310.

Owens, W. H. 1974b. Mathematical model studies on factors affecting the magnetic anisotropy of deformed rocks. *Tectonophysics* **24**, 115–131.

Owens, W. H. & Bamford, D. 1976. Magnetic, seismic and other anisotropic properties of rock fabrics. *Phil. Trans. R. Soc. Lond. A* **283**, 55–68.

Peach, B. N., Horne, J., Gunn, W., Clough, C. T. & Hinxman, L. W. 1907. The geological structure of the north-west Highlands of Scotland. *Mem. Geol. Surv. U.K.*

Siddans, A. W. B. 1976. Deformed rocks and their textures. *Phil. Trans. R. Soc. Lond.* A **283**, 43–54

Stacey, F. D. 1960. Magnetic anisotropy of igneous rocks. *J. Geophys. Res.* **65**, 2429–2442.

Wood, D. S., Oertel, G., Singh, J. & Bennett, H. F. 1976. Strain and anisotropy in rocks. *Phil. Trans. R. Soc. Lond.* A **283**, 27–42.

APPENDIX

Description of specimens 1 *to* 8

Specimens 1 to 3 are from the flat, right way up, limb of the Lochalsh fold. They are medium grained, pale brown sandstones. Quartz grains are sub-angular to rounded and there are numerous detrital feldspars. Some of the quartz grains have sutured margins, they show undulose extinction and small sub-grains. Some grains are fractured. Micas occur along the grain margins though no preferred orientation of mica could be detected under the microscope. Opaque minerals occur along some grain margins and also along cracks in the quartz grains. Figure 4(a) shows a section of specimen 3.

Specimen 4 is of fine grained pale brown sandstone – siltstone. The original quartz grains are well preserved and show a slight elongation. The quartz grain margins are often pitted suggesting a solution process. The grains also show undulose extinction and are occasionally fractured. Micas, locally with opaque minerals, rim the detrital grains. Some micas occur in a fibrous form, parallel to the grain elongation direction. Similar orientated micas infill cracks in the grains. The orientations of bedding and cleavage are shown in Fig. 13(a).

Specimen 5 is of grey sandstone. It shows similar textures to that of specimen 4 but the grain size is larger and there is less mica. There is a good grain shape fabric and the long axis of the grain fabric ellipsoid plunges to the SE. Figure 4(b) shows a section of this specimen.

Specimen 6 is of a grey shale which shows a good grain shape fabric. Zones rich in mica define the cleavage, though individual micas are oblique to these zones. Elongate quartz grains also define a fabric which predates the main cleavage.

Specimens 7 and 8 were originally sandstones. The original grains are just identifiable under the microscope though they are largely a mass of sub-grains and new grains. Micas occur in pressure shadows at the end of more rigid feldspar grains, they occupy cracks in detrital feldspar and quartz grains and also rim the small new grains.

Details of the magnetic anisotropy of these specimens are given in Table 2. Only in specimens 1 and 8 was it possible to separate the linear and saturation components of the magnetisation.

Table 2. Details of the magnetic anisotropy of specimens 1 to 8, described in Fig. 5 and the Appendix. Anisotrophy measurements taken at 5 kOe. Linear and saturating components separated only for specimens 1 and 8.

Specimen	Rock type	Grain shape ratio/fabric	Hs	V	X	Y	Z
1	Sandstone	No detectable fabric	0.083	–0.052	109/33	235/41	356/30
1 (linear)					091/20	221/49	345/26
1 (saturating)					145/04	023/80	236/07
2	Sandstone	No detectable fabric	0.115	–0.107	311/40	095/43	204/19
3	Sandstone	No detectable fabric	0.383	–0.052	324/59	117/27	213/01
4	Siltstone/shale	Weak Cleavage	0.138	0.040	120/16	022/24	240/59
5	Sandstone	3.5 : 1.97 : 1	0.142	0.475	125/05	214/04	009/84
6	Siltstone	Not measured	0.262	0.620	084/22	181/17	305/61
7	Sandstone	Original grains obliterated	0.129	–0.059	120/09	210/00	300/80
8	Sandstone	Original grains obliterated	0.127	–0.002	046/18	136/01	232/71
8 (linear)					044/14	136/04	244/74
8 (saturating)					047/22	137/00	230/67